InP/InGaAsP Flattened Ring Lasers With Low-Loss Etched Beam Splitters

John S. Parker, Erik J. Norberg, Yung-Jr Hung, Byungchae Kim, Robert S. Guzzon, and Larry A. Coldren, *Fellow, IEEE*

Abstract—Compact flattened InP/InGaAsP multiquantum-well (MQW) resonators based on etched beam splitters (EBS) with 300- to 800-nm gaps and circumferences of 30–300 μm are demonstrated. Comparison of the EBS coupler reflection and transmission to 3-D finite-difference time-domain (FDTD) simulations shows good agreement in the wider EBS gap devices. Lasing is observed in 90-, 150-, and 300-μm length rings at threshold currents of 15, 14, and 29 mA, respectively.

Index Terms—Beam splitter, integrated optics, optical resonators, photonic integrated circuits.

I. INTRODUCTION

COMPACT integrated ring resonators can provide diverse functionality in photonic integrated circuits (PICs) due their multitude of uses as delay lines [1], programmable memory elements [2], optical switches [3], optical filters [4] tunable lasers [5], and biological sensors [6]. Ring resonators have been demonstrated with several geometries including: standard circular rings [2], racetrack resonators [3], rectangular rings [7], and flattened rings [8]. The flattened ring design uses a larger bending radius with arcs covering $\sim 120°$ and two etched beam splitters (EBS) to provide the remaining 240° necessary to complete the loop. Increasing the bending radius decreases the scattering losses, which becomes significant in small rings. Therefore, the use of flattened rings with EBS couplers can enable lower loss compact cavities.

EBS couplers are based on frustrated total internal reflection (FTIR), using a low refractive index trench to separate two etched mirrors [9]. The couplers are designed for an incident angle greater than the critical angle (i.e., for the In/InGaAsP material platform the critical angle is 18° for an air-trench [8], or higher for a trench filled with dielectric such as Benzocyclobutane [10]). As the incident optical mode is reflected by the trench, the evanescent field couples a portion of the modal power across the low index gap. Semiconductor based EBS, also known as FTIR couplers, were first demonstrated in 1987 on the GaAs/AlGaAs material platform using an ion milled air trench

[11]. Recently, demonstrations of EBS couplers have been realized in Si [12], GaAs/AlGaAs [13], and InP/InGaAsP [8], [10]. The compact size of the EBS provides the capability to create small devices. The minimum size of ring resonators is ultimately limited by the coupler length. As an example, for ultra-compact InP designs realized by lithography, the minimum length demonstrated is 55 μm for a directional coupler [14], 20 μm for a multimode interference (MMI) coupler [15], and 8 μm for an etched beam splitters [8].

We present EBS couplers designed with low insertion loss for use in compact ring lasers, and the smallest flattened ring cavities yet reported with circumference of 30 μm and a cavity footprint of 8 μm $\times$ 20 μm. For these compact photonic devices, ease of integration is vital for combining components with diverse functionality on a single PIC. To address this, we have developed a fabrication process for defining waveguides and 300 nm EBS trenches using a single i-line (365 nm source) photolithographic exposure. Furthermore, the waveguides and trenches are created in one dry etch by using an SiO_2 etch delay mask for the waveguides. Previous studies have used expensive electron-beam-lithography (EBL) for narrow trench definition [9], [10], [12], [13]. Using only stepper lithography, we demonstrate that narrow EBS trenches can be realized on PICs with relatively low added cost for integration of compact flattened ring lasers with other deeply etched components.

II. FABRICATION

The device is fabricated on an InP/InGaAsP centered quantum well (CQW) platform with 10 compressively strained QWs sandwiched in-between two 105 nm 1.3Q InGaAsP layers. Passive waveguides are defined by an intermixing process of phosphorous implantation and rapid thermal annealing at 675°C to shift the bandgap of the CQWs from 1545 nm to 1410 nm. A single blanket regrowth is used to cover the device with a 1.8 μm p-InP cladding and p-InGaAs contact layer.

A bilayer Cr/SiO_2 (50/650 nm) hardmask and a single lithographic exposure are used to define the waveguides and EBS couplers to avoid any angular misalignment between the coupler and the waveguide. The photolithography is done using a GCA Autostep200 stepper with a numerical aperture of 0.45. The photoresist (PR) used is 200 nm thick THMR-M100 with 300 nm thick contrast enhancer CEM365iS. The thin PR was necessary to define 300 nm gaps for the smallest EBS as shown by the scanning electron microscope (SEM) image in Fig. 1(a). A diagram of this ring is shown in Fig. 1(b).

The Cr was etched in a low power Cl_2 based inductively coupled plasma (ICP), the PR removed, and 550 nm out of the 650 nm of SiO_2 was etched in a SF_6 based ICP. An additional 40 nm of Cr was deposited and defined by liftoff to cover the
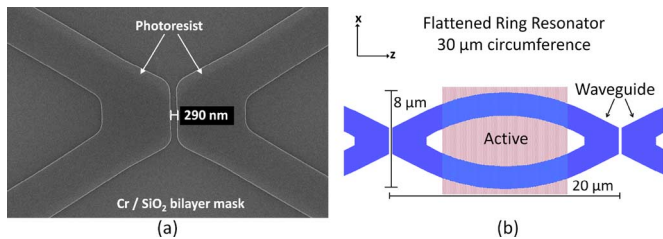
Fig. 1. (a) Scanning electron microscope image of the photoresist after waveguide and EBS trench have been defined (290-nm measured gap). (b) Diagram of 30-μm circumference flattened ring (top view).
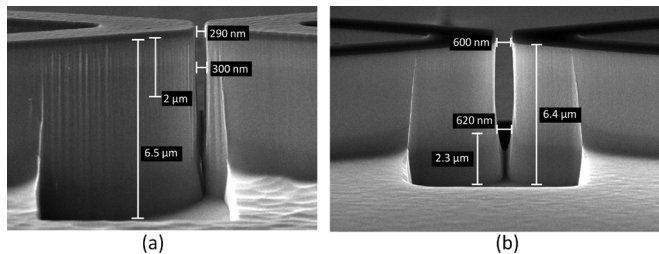

Fig. 2. SEM images of deeply etched waveguides and trenches with gap sizes of (a) 300 nm and (b) 600 nm. A SiO$_2$ etch delay allows the EBS trench to etch for longer than the waveguides to account for the RIE lag effect in the high aspect-ratio trench.
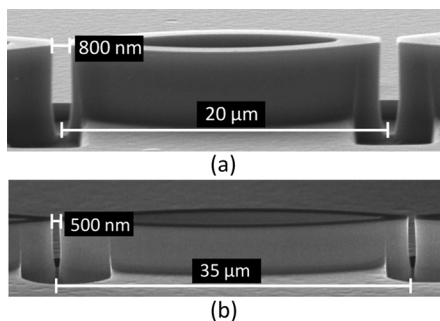

Fig. 3. SEM images of flattened ring resonators with circumferences of (a) 30 μm and (b) 60 μm, with EBS couplers on both sides.

waveguides outside the EBS. This Cr served as a mask to etch the remaining 100 nm of SiO$_2$ inside the EBS regions. The Cr was removed prior to InP etching and the final SiO$_2$ mask provided a 100-second etch delay for the waveguides. This delay helps account for the difference in etch speed in the narrow EBS trench due to the RIE lag effect, which reduces the etch rate in small features. The InP/InGaAsP was deeply etched in a Unaxis ICP reactive ion etch (RIE) with Cl$_2$/H$_2$/Ar chemistry and a 200°C heated chuck. From Fig. 2, the etch depth was 5 μm for the waveguides and 6.5 μm inside the EBS regions. The benefit of this SiO$_2$ lag mask etching technique was that it allowed two etch depths to be achieved in a single dry etch. Previous multilevel dry etches have required multiple etches, which caused undesirable sidewall kinks [7].

A 30 μm and a 60 μm circumference flattened ring are shown in Fig. 3 after dry etching. The finished devices have ohmic Pt/Ti/Pt/Au contacts evaporated on the p-InGaAs layer and Ti/Au contacts on the backside of the InP:S substrate.

III. LASING RESULTS

The 90, 150, and 300 μm circumference rings lase at threshold currents of 15, 14, and 29 mA respectively. No unidirectional lasing or bistability was observed. The lasing spectra for the three resonators are shown in Fig. 4. The shift
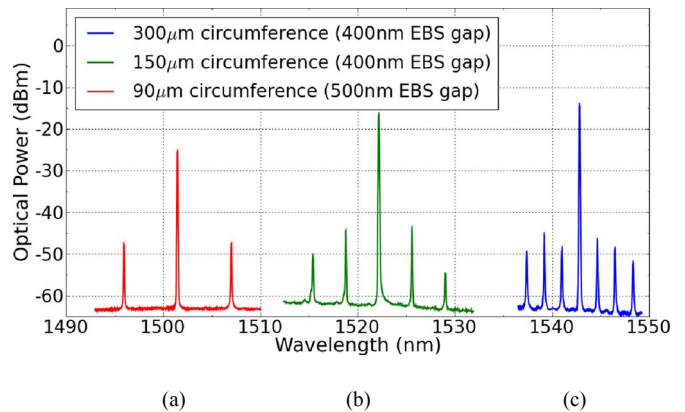

Fig. 4. Optical spectra of flattened ring lasers with circumferences of (a) 90 μm, (b) 150 μm, and (c) 300 μm. The shift in lasing wavelength is due to partially intermixed quantum wells at the edge of the active region.

in lasing wavelength for the shorter rings was due to partial intermixing at the edge of the active region. As the ring length is decreased, the effects at the edge of the active region become more significant. In future devices, the implant and intermixing process will need to be optimized for a sharper transition to minimize these edge effects.

Rings with 30 μm and 60 μm circumference did not lase, however they did produce pole filter responses with extinction ratios of 4 and 5.5 dB respectively, hence, these resonators can be used in wide bandwidth and channelizing applications. The free spectral range (FSR) of the resonators varied from 13 nm for the 30 μm ring to 1.8 nm for the 300 μm ring.

IV. EBS COUPLER RESULTS AND SIMULATIONS

Three-dimensional finite-difference time-domain (FDTD) method simulations using Rsoft software with optical power monitors were used to study the EBS reflection and transmission properties. The 3-D-FDTD provided more accurate simulations for EBS losses than the 2-D-FDTD, due to significant transverse diffraction for which the 2-D-FDTD does not account.

The devices were built and tested for TE polarized light only, as the compressively strained InGaAsP QWs have a large TE gain and a small TM gain. The peak measured gain of the semiconductor optical amplifiers (SOAs) was 50 dB/mm. From this we calculated that the 30 μm ring had only 1.5 dB of gain per cavity round-trip. With such small net gain, minimizing insertion loss was crucial to realize compact filters and lasers. For this reason, the EBS couplers were designed for large incident angles of 30° to 32° to reduce insertion loss for the compact ring lasers. As shown in Fig. 5, simulated insertion loss decreases from 1 dB to 0.2 dB by increasing the incident angle from 20° to 32°.

To measure the insertion loss of the EBS coupler, a separate test structure as outlined in Fig. 6(a) is utilized. By fiber coupling a tunable laser, the optical power is recorded by an on-chip reverse biased SOA detector at the EBS input. Once the coupled-in optical power is determined, the detector is forward biased at its transparency current and the EBS reflection and transmission are measured by on-chip detectors. The measured insertion loss at 32° incident angle is 0.6 $\pm$ 0.5 dB. The
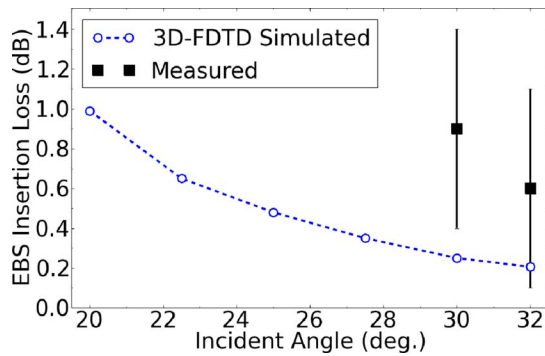
Fig. 5. Measurements and 3-D finite-difference time-domain simulations of the EBS coupler insertion loss versus incident angle for a 400-nm air gap.
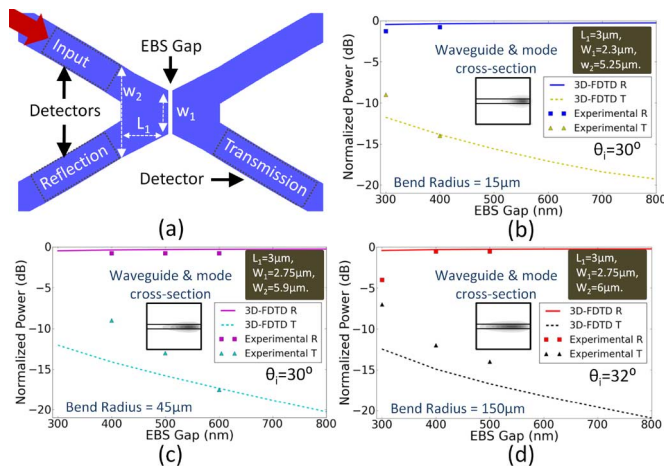

Fig. 6. (a) Schematic of trench test setup using an external tunable laser input and on-chip detectors on all ports. The input detector is used to measure the power coupled on-chip and then forward biased at transparency to test trench reflection (R) and transmission (T). Measured data and 3-D-FDTD coupling simulations for ring circumferences of (b) 30 μm, (c) 90 μm, and (d) 300 μm.

uncertainty occurs due to variation in the SOA transparency currents.

Simulations and experimentally measured values for reflection and transmission of the 30, 90, and 300 μm circumference rings are shown in Fig. 6. The wider gap EBS devices show the best agreement with the simulations. This is likely due to nonvertical trench sidewalls on the smaller EBS gaps. As shown in Fig. 2(a), the gap at the waveguide layer ($\sim 2 \mu$m below the top layer) is narrower than the gap on the mask and has a nonvertical sidewall angle. These deviations results in higher transmission, due to the narrower gap, and increased insertion loss due to the nonvertical sidewall.

Variations to the EBS design were made for each bending radii to account for the differences in modal shape in the tightly curved waveguides. For tight bends, the mode is squeezed towards the outside of the waveguide. To accommodate this mode profile, the coupler width is reduced in devices with tighter bending radius as shown in Fig. 6(b)–(d). Unlike previous EBS couplers for straight and large radius of curvature waveguides that used a wide multimode platform region around the EBS trench [8], [10], the current design uses a "restricted" beam splitter keeping the mode highly confined up to the trench similar to work done in GaAs/AlGaAs [11]. The restricted EBS is

necessary for bending radius $\leq 150 \mu$m to prevent excitation of higher-order-modes as the tight bending radius transitions to the straight beam splitter.

V. CONCLUSION

We have demonstrated compact flattened ring resonators down to 30 μm circumference with free spectral range of 13 nm. A novel process, using an etch delay mask, created deeply etched waveguides and air trenches in a single etch. The EBS couplers were designed with incident angles $\geq 30°$ to minimize insertion losses for small rings with tight bending radii. Compact flattened rings are promising devices for use in the next generation of PICs as integrated lasers and WDM filters.

REFERENCES

[1] F. Morichetti, A. Melloni, C. Ferrari, and M. Martinelli, "Error-free continuously-tunable delay at 10 Gbit/s in a reconfigurable on-chip delay-line," *Opt. Express*, vol. 16, no. 12, pp. 8395–8405, 2008.

[2] M. T. Hill, H. J. S. Dorren, T. de Vries, X. J. M. Leijtens, J. H. de Besten, B. Smalbrugge, Y. S. Oei, H. Binsma, G. D. Khoe, and M. K. Smit, "A fast low-power optical memory based on coupled micro-ring lasers," *Nature*, vol. 432, pp. 206–209, 2004.

[3] T. A. Ibrahim, R. Grover, L. C. Kuo, S. Kanakaraju, L. C. Calhoun, and P. T. Ho, "All-optical AND/NAND logic gates using semiconductor microresonators," *IEEE Photon. Technol. Lett.*, vol. 15, no. 10, pp. 1422–1424, Oct. 2003.

[4] E. J. Norberg, R. S. Guzzon, S. C. Nicholes, J. S. Parker, and L. A. Coldren, "Programmable optical lattice filter in InGaAsP–InP," *IEEE Photon. Technol. Lett.*, vol. 22, no. 2, pp. 109–111, Jan. 15, 2010.

[5] Y. Ki-Hong, R. O. Kwang, K. S. Ki, H. K. Jong, and C. K. Dong, "Monolithically integrated tunable laser using double-ring resonators with a tilted multimode interference coupler," *IEEE Photon. Technol. Lett.*, vol. 21, no. 13, pp. 851–853, Jul. 1, 2009.

[6] A. Yalcin, K. C. Popat, J. C. Aldridge, T. A. Desai, J. Hryniewicz, N. Chbouki, B. E. Little, O. King, V. Van, S. Chu, D. Gill, M. Anthes-Washburn, M. S. Unlu, and B. B. Goldberg, "Optical sensing of biomolecules using microring resonators," *IEEE J. Sel. Topics Quantum Electron.*, vol. 12, no. 1, pp. 148–155, Jan./Feb. 2006.

[7] R. Zhang, Z. Ren, and S. Yu, "Fabrication of InGaAsP double shallow ridge rectangular ring laser with total internal reflection mirror by cascade etching technique," *IEEE Photon. Technol. Lett.*, vol. 19, no. 21, pp. 1714–1716, Nov. 1, 2007.

[8] E. J. Norberg, J. S. Parker, U. Krishnamachari, R. S. Guzzon, and L. A. Coldren, "InP/InGaAsP based flattened ring resonators with etched beam splitters," in *Proc. Integrated Photonics and Nanophotonics Research and Applications*, Honolulu, HI, 2009, Paper IWA1.

[9] N. R. Huntoon, M. P. Christensen, D. L. MacFarlane, G. A. Evans, and C. S. Yeh, "Integrated photonic coupler based on frustrated total internal reflection," *Appl. Opt.*, vol. 47, pp. 5682–5690, 2008.

[10] B. Kim and N. Dagli, "Compact bandstop filters with semiconductor optical amplifier, etched beam splitters and total internal reflection mirrors," in *Proc. Integrated Photonic Research*, Monterey, CA, 2010, Paper ITuC6.

[11] J. S. Osinski, C. E. Zah, R. Bhat, R. J. Contolini, E. D. Beebe, and T. P. Lee, "Miniature integrated optical beam-splitter in AlGaAs/GaAs ridge waveguides," *Electron. Lett.*, vol. 23, no. 21, pp. 1156–1158, 1987.

[12] Y. Qian, J. Song, S. Kim, and G. P. Nordin, "Compact 90° trench-based splitter for silicon-on-insulator rib waveguides," *Opt. Express*, vol. 15, pp. 16712–16718, 2007.

[13] B. Kim and N. Dagli, "Submicron etched beam splitters based on total internal reflection in GaAs–AlGaAs waveguides," *J. Lightw. Technol.*, vol. 28, no. 13, pp. 1938–1943, Jul. 1, 2010.

[14] Y. Shi, S. He, and S. Anand, "Ultracompact directional coupler realized in InP by utilizing feature size dependent etching," *Opt. Lett.*, vol. 33, no. 17, pp. 1927–1929, 2008.

[15] Y. Ma, S. Park, L. Wang, and S. T. Ho, "Ultracompact multimode interference 3-dB coupler with strong lateral confinement by deep dry etching," *IEEE Photon. Technol. Lett.*, vol. 12, no. 5, pp. 492–494, May 2000.